CHEMISTRY OF MATERIALS

Article

pubs.acs.org/cm

Systematic Investigation of Isoindigo-Based Polymeric Field-Effect Transistors: Design Strategy and Impact of Polymer Symmetry and Backbone Curvature

Ting Lei, Yue Cao, Xu Zhou, Yang Peng, Jiang Bian, and Jian Pei*

Beijing National Laboratory for Molecular Sciences, the Key Laboratory of Bioorganic Chemistry and Molecular Engineering of Ministry of Education, College of Chemistry and Molecular Engineering, Peking University, Beijing 100871, China

Supporting Information

ABSTRACT: Ten isoindigo-based polymers were synthesized, and their photophysical and electrochemical properties and device performances were systematically investigated. The HOMO levels of the polymers were tuned by introducing different donor units, yet all polymers exhibited *p*-type semiconducting properties. The hole mobilities of these polymers with centrosymmetric donor units exceeded 0.3 $cm^2\ V^{-1}\ s^{-1}$, and the maximum reached 1.06 $cm^2\ V^{-1}\ s^{-1}$. Because of their low-lying HOMO levels, these copolymers also showed good stability upon moisture. AFM and GIXD analyses revealed that polymers with different symmetry and backbone curvature were distinct in lamellar packing and crystallinity. DFT calculations were employed to help us propose the possible packing model. Based on these results, we propose a design strategy, called "molecular docking", to understand the interpolymer $\pi-\pi$ stacking. We also found that polymer symmetry and backbone curvature affect interchain "molecular docking" of isoindigo-based polymers in film, ultimately leading to different device performance. Finally, our design strategy maybe applicable to other reported systems, thus representing a new concept to design conjugated polymers for field-effect transistors.

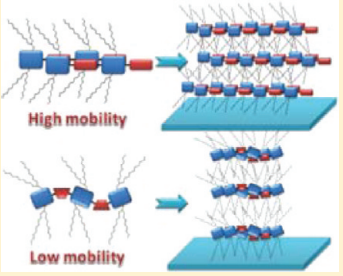

KEYWORDS: *polymeric field-effect transistors, structure–property relationship, conjugated polymers, organic electronics*

INTRODUCTION

Organic field-effect transistors (OFETs) are advancing rapidly in terms of their applications in low-cost, large-area thin film transistors.[1] Compared to small molecules, polymers offer great advantages, such as solution processability, good mechanical property, and thermal stability.[2] Benefiting from new molecular design and device fabrication improvement, polymeric field-effect transistors (PFETs) have made significant progress in past decade and some of them exhibit carrier mobility approaching or surpassing 1 $cm^2\ V^{-1}\ s^{-1}$.[3] However, upon prolonged exposure to air or moisture, device performance degradation is also a critical problem for practical application of PFETs.[4] With notably rare exceptions,[3a,c,5c,d] PFETs with high carrier mobility and long-time stability are usually achieved in low-humidity and inert atmosphere.[4] Therefore, to design new polymers for high-mobility PFETs with ambient stability is still of great challenge.[5] On the other hand, the structure–property relationship is important for designing new organic materials for optoelectronics. Although several design strategies and even computational methods have been proposed for small molecular OFETs,[6−9] rational design strategy for PFETs are seldom reported.

Herein, employing the concept of molecular docking, we design and synthesize ten copolymers for PFETs to investigate their structure–property relationship (Figure 1). In the molecular modeling field, docking is a method to predict the structure of intermolecular complex formed between two or more constituent molecules.[10] Molecular docking has been broadly used to understand the biological processes determined by noncovalent interactions, especially for rational design of drugs.[11] Electron-deficient unit, isoindigo, with branched alkyl chains as acceptor, and ten different electron-rich units as donor are combined to prepare ten isoindigo-based copolymers. Because of the donor–acceptor interaction and the spatial steric hindrance caused by the branched alkyl chains, we envision that the small units dock into the cavity formed by the isoindigo cores and branched alkyl chains (Figure 1c). We systematically compare FET device performances, polymer packings and film morphologies of the polymers, and find that this strategy is efficient to obtain high-performance FETs. Polymers with centrosymmetric donors exhibit systematically higher field-effect mobility than those with axisymmetric ones. By means of atomic force microscopy (AFM) and grazing-incident X-ray diffraction (GIXD), we attribute the great difference in device performance to the different symmetry and backbone curvature of the polymers, which greatly affect the interpolymer docking and lamellar packing. Density functional theory (DFT) calculations support our proposed packing model. Finally, we compare the device performances of diketopyrrolopyrole (DPP) and naphthalenedicarboximide

Received: January 11, 2012
Revised: April 26, 2012
Published: May 2, 2012

   dx.doi.org/10.1021/cm300117x | *Chem. Mater.* 2012, 24, 1762–1770

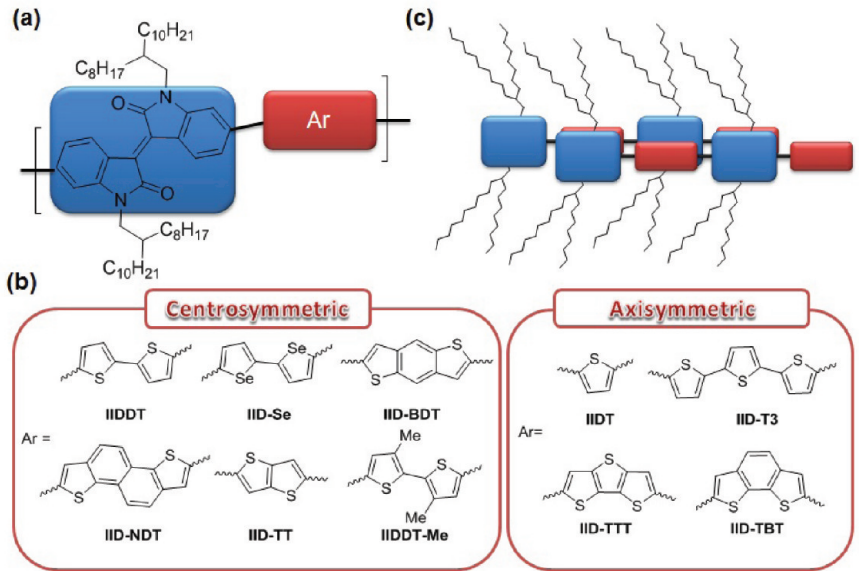

Figure 1. (a) Structures of isoindigo-based copolymers; (b) centrosymmetric and axisymmetric donor of the copolymers; (c) proposed interpolymer docking model.

Scheme 1. Synthesis of Monomers and Isoindigo-Based Copolymers.[a]

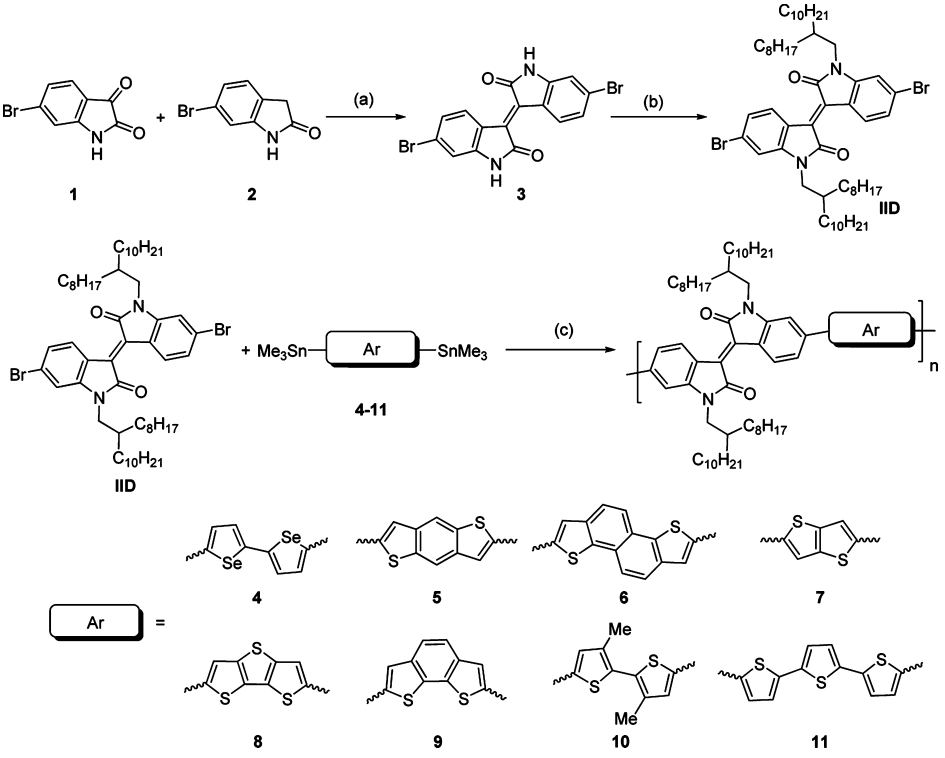

[a]Reagent and conditions: (a) AcOH/HCl, reflux, 24 h, 86%; (b) 1-iodo-2-octyldodecane, K_2CO_3, DMF, 74%; (c) $Pd_2(dba)_3$, P(*o*-tol)$_3$, toluene, 110 °C, 48 h.

(NDI) based polymers reported by other groups, and we conclude that the molecular docking strategy is also applicable to those systems, and thus representing a new concept to design conjugated polymers for PFETs.

RESULTS AND DISCUSSION

Design and Synthesis. Electron-deficient isoindigo unit is a new building block for low bandgap polymeric solar cells.[12] As isoindigo homopolymer is a typical *n*-type semiconductor,[13] in order to obtain *p*-type isoindigo-based polymers, electron-rich groups should be introduced to increase the HOMO level of the desired polymers. The donor−acceptor interactions of electron-deficient isoindigo skeleton and electron-rich units enhance the interchain $\pi-\pi$ stacking.[14,15] Selenophene- (**4**) and thiophene-containing (**5**−**11**) units were employed to construct these copolymers (Scheme 1). Units **4**−**7** and **10** are centrosymmetric, and units **8**, **9**, and **11** are axisymmetric. To prove our molecular docking strategy, we also synthesized 3,3′-

dx.doi.org/10.1021/cm300117x | *Chem. Mater.* 2012, 24, 1762−1770

dimethyl-2,2′-bithiophene (**10**) to compare with 2,2′-bithiophene. We envision that the methyl groups may hinder $\pi-\pi$ stacking and interchain docking. Compounds **4**,[3b] **5**,[16] **6**,[17] **7**,[18] **8**,[19] and **9**[20] were synthesized according to literatures. Monomer **IID** were obtained from commercially available 6-bromoisatin (**1**) and 6-bromooxindole (**2**) only two steps with high yield. All monomers were prepared in 10-g scale. The copolymers were obtained through Stille-coupling polymerization using $Pd_2(dba)_3$ and P(*o*-tol)$_3$ as catalysts. After the polymerization, strongly complexing ligand *N*,*N*-diethylphenylazothioformamide was added to remove any residual catalyst. All polymers were purified by Soxhlet extraction (sequentially by methanol, hexane, and $CHCl_3$), and afforded dark or dark blue solids. After introducing the branched alkyl chains, all polymers (except **IID-T3**) showed good solubility in common solvents, such as $CHCl_3$, toluene, and THF. **IID-T3** dissolved in chloro-containing solvents such as $CHCl_3$, trichloroethylene (TCE), and dichlorobenzene (DCB).

Molecular weights of all polymers were evaluated by gel permeation chromatography (GPC) using 1,2,4-tricholorobenzene (TCB) as eluent at 150 °C. Large PDI remained at 150 °C, presumably because of strong aggregation of the polymers by strong interchain interactions. All polymers showed good thermal stability with decomposition temperatures over 350 °C. No phase transition was observed by differential scanning calorimetry (DSC) before decomposition.

Photophysical and Electrochemical Properties. The absorption spectra of all polymers in dilute solution, in thin film and in annealed film are shown in Figure 2 and Figure S1 in the Supporting Information. All polymers show typically dual band absorption both in solution and in film: band I (500−800 nm) and band II (300−500 nm). Varying with different polymers, band II was attributed to the absorption of the donor part. In contrast, these polymers had similar features in band I region with three obvious vibrational peaks 0−0, 0−1, and 0−2, thus associating the shape-persistent isoindigo core. In addition, band I is a typical charge-transfer absorption from the donor part to the isoindigo core. After introducing relatively weak donors, benzodithiophene (BDT) and naphtho[1,2-b:5,6-b′]dithiophene (NDT), **IID-BDT** and **IID-NDT** showed obvious blue-shift of the absorption spectra compared with other polymers. Computational results show that the HOMOs are well delocalized along the polymer chain, but the LUMOs are mostly localized on the isoindigo core (Figure 3a).

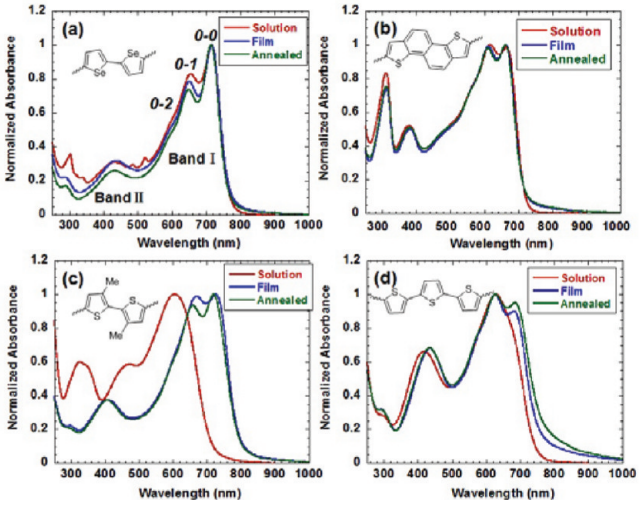

Figure 2. Normalized UV−vis absorption spectra of (a) **IID-Se**, (b) **IID-NDT**, (c) **IIDDT-Me**, and (d) **IID-T3** in $CHCl_3$ (1×10^{-5} M), in thin film (spin-cast from TCE solution, 1 mg/mL), and in annealed film (150 °C for 30 min).

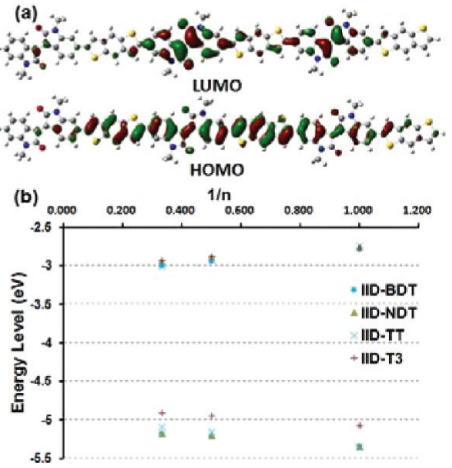

Figure 3. (a) Calculated molecular orbitals of the **IID-BDT** trimer; (b) HOMO and LUMO energy levels are calculated for oligomers (n = 1, 2, and 3) of **IID-BDT**, **IID-NDT**, **IID-TT**, and **IID-T3**. The energy levels of polymers can be extrapolated from the values. Alkyl chains are replaced with methyl groups for computational simplicity, and all the calculations are performed at B3LYP/6-31G (d) levels.

The absorption peaks of all polymers (except for polymer **IIDDT-Me**) in film showed no obvious red-shift in comparison with those in solution. This suggests that the polymers adopted similar geometry both in solution and in film. Scrutiny of spectra reveals that the 0−0 vibrational transition increased, whereas 0−1 decreased in film, suggesting that polymers become more planar or form some *J* aggregates in film. After annealing the film at 150 °C for 30 min, a further increase of the 0−0 transition was observed, indicating the packing and planarity of polymers were improved. Two methyl groups of **IIDDT-Me** resulted in a great torsion angle, which broke the conjugation, thus leading to an obvious blue-shift in solution. This torsion angle was suppressed in solid state because of interchain $\pi-\pi$ stacking, hence red-shifting the absorption maximum significantly (over 100 nm) to a similar region as other polymers (Table 1).

The cyclic voltammetries (CV) of all polymers in thin films were measured to evaluate their electronic energy levels (Figure 4 and Figure S2 in the Supporting Information). Most polymers showed much stronger oxidative peaks than reductive ones, almost 1 order of magnitude higher, which indicated that these polymers were more easily oxidized. All polymers showed similar reductive potentials with LUMO levels around −3.70 eV. HOMO levels of polymers vary with electron-donating properties of donor units. For example, the HOMO/LUMO level of **IID-Se** is −5.65/−3.79 eV, and that of **IID-TT** is −5.70/−3.73 eV. Polymers containing less weak donors had lowered HOMO levels (−5.84 eV for **IID-BDT** and −5.90 eV for **IID-NDT**). These results were consistent with the calculation that LUMO levels of all polymers were mostly localized on the isoindigo core and HOMO levels were distributed along the polymer chains (Figure 3a). Thus HOMO levels of all polymers were more easily affected by the electronic structure of the donor unit, whereas the LUMO levels remained

dx.doi.org/10.1021/cm300117x | *Chem. Mater.* 2012, 24, 1762−1770

Table 1. Optical and Electrochemical Properties of Polymers

polymers	M_n (kDa) /PDI[a]	λ_{max}^{0-0} sol (nm)[b]	λ_{max}^{0-1} sol (nm)[b]	λ_{max}^{0-0} film (nm)[c]	λ_{max}^{0-1} film (nm)[c]	E_g^{opt} (eV)[d]	E_{HOMO} (eV)[e]	E_{LUMO} (eV)[e]	E_g^{cv} (eV)[f]
IIDDT	33.7/5.4	706	647	701	637	1.59	−5.65	−3.78	1.87
IID-Se	26.7/3.5	716	655	715	649	1.56	−5.56	−3.79	1.77
IID-BDT	27.3/4.7	674	646	676	620	1.66	−5.84	−3.77	2.07
IID-NDT	24.8/3.5	666	616	662	610	1.69	−5.90	−3.75	2.15
IID-TT	25.5/3.5	723	666	720	656	1.55	−5.70	−3.73	1.97
IIDDT-Me	20.1/3.9	604	N.A.	725	670	1.54	−5.54	−3.78[g]	1.76
IIDT	19.6/3.1	691	644	697	645	1.58	−5.80	−3.81	1.99
IID-T3	38.8/3.4	N.A.	628	682	628	1.58	−5.48	−3.70[g]	1.78
IID-TTT	26.6/3.7	719	662	720	656	1.55	−5.44	−3.72	1.73
IID-TBT	11.2/2.5	658	613	668	615	1.65	−5.55	−3.70	1.85

[a]GPC versus polystyrene standards, TCB as eluent, at 150 °C. [b]Solution absorption spectra (1×10^{-5} M in chloroform). [c]Thin film absorption spectra from pristine film spin-cast from 5 mg/mL TCE solution. [d]Optical energy gap estimated from the onset of the film absorption. [e]cyclic voltammetries were determined with Fc/Fc^+ ($E_{HOMO} = -4.80$ eV) as external reference. [f]$E_g^{CV} = E_{LUMO} - E_{HOMO}$. [g]The first reduction peak was weak.

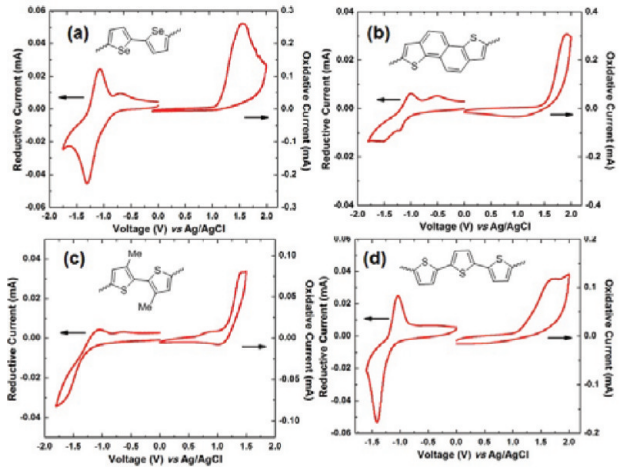

Figure 4. Cyclic voltammogram of (a) **IID-Se**; (b) **IID-NDT**; (c) **IIDDT-Me**; and (d) **IID-T3** in thin film drop-casting on a glassy carbon electrode and tested in n-Bu_4NPF_6/CH_3CN solution (scan rate: 50 mV s^{-1}).

unchanged. Interestingly, **IID-TTT** showed two oxidative peaks and a HOMO level of −5.44 eV, indicating the strong electron-donating property of dithieno[3,2-b:2′,3′-d]thiophene (see the Supporting Information). Using DFT calculation, we obtained theoretical HOMO/LUMO levels of polymers by extrapolating the calculated energy levels of oligomers (n = 1−3) (Figure 3b). Although DFT calculations usually provide higher values than electrochemical results, both methods gave similar trends of energy-level variations. As shown in Figure 3b, the HOMO level of **IID-T3** was much higher than those of other polymers and that of **IID-TT** was relatively higher than those of **IID-BDT** and **IID-NDT**. However, their LUMO levels showed no obvious change. All photophysical and electrochemical data are summarized in Table 1.

Field-Effect Transistor Fabrication and Characterization. Bottom-gate/top-contact (BG/TC) devices were fabricated by spin-coating the polymer solutions (4 mg/mL) onto octadecyltrimethoxysilane (OTS) treated SiO_2 (300 nm) on heavily doped Si substrate. Previously, we used TCE as solvent to fabricate thin film transistors. After optimizing conditions, we found that using TCB provided better device performance. For example, with TCE as solvent, **IIDDT** only gave an average hole-mobility of 0.42 cm^2 V^{-1} s^{-1}, whereas with TCB a maximum mobility up to 1.06 cm^2 V^{-1} s^{-1} and average mobility of 0.66 cm^2 V^{-1} s^{-1} were obtained (Figure 5a). This result is among the highest values reported to date. Use of TCB as solvent to improve PFETs device performance was also reported in the fabrication of P3HT based device, because TCB with high boiling point provided P3HT with better interchain packing and more condensed uniform film.[21,22] Because the OTS treated SiO_2 surface is very hydrophobic and TCB has a relatively higher contact angle than TCE, spin-coating on the surface was only achieved for polymers **IIDDT**, **IID-Se**, or **IID-NDT** in TCB, presumably because of their higher molecular weight and viscosity. For other polymers, spin-coating from their TCB solutions did not provide continuous films. We also found that solvent-annealing in TCE atmosphere in Petri dish effectively improved the device performance after spin-coating from TCE solutions. Thus solvent-annealing with TCE in Petri dish was also performed for polymers after spin-coating from TCE. To our delight, all polymers with centrosymmetric donors showed excellent hole-transporting properties with mobilities over 0.1 cm^2 V^{-1} s^{-1}. (Figure 5, Table 2). Such systematically high mobilities rarely appeared in literature. Although selenophene-containing polymers were reported to show a better carrier-transporting performance in OFETs than that of the thiophene-containing polymers,[3b] our selenophene-containing polymer **IID-Se** only showed a comparable result with that of the thiophene-containing polymer **IIDDT** (with the maximum hole mobility up to 0.66 cm^2 V^{-1} s^{-1} and average mobility of 0.46 cm^2 V^{-1} s^{-1}). **IIDDT-Me** showed the worst performance (with the maximum hole mobility of 0.11 cm^2 V^{-1} s^{-1} and average mobility of 0.091 cm^2 V^{-1} s^{-1}), about 1 order of magnitude lower than that of **IIDDT**. Methyl groups hinder the interchain $\pi-\pi$ stacking and thereby reduce the mobility. In sharp contrast, all polymers with axisymmetric donors showed much lower hole mobilities (see Figure S3 in the Supporting Information). **IIDT** had a maximum hole-mobility of 0.019 cm^2 V^{-1} s^{-1}, and **IID-T3** had a maximum hole-mobility of 0.061 cm^2 V^{-1} s^{-1}. **IID-TTT** and **IID-TBT** showed poor hole-mobility in the range of 1×10^{-3} to 1×10^{-4} cm^2 V^{-1} s^{-1}.

Oxidative potentials of polymers correlate the threshold voltages of their devices. **IID-Se** and **IID-TT** have higher HOMO levels than **IIDDT**, and their threshold voltage were more positive (−10 V for **IID-Se** and −6 V for **IID-TT**). Similarly, **IID-BDT** and **IID-NDT** have lower HOMO levels and their threshold voltages were more negative (−28 V for

dx.doi.org/10.1021/cm300117x | Chem. Mater. 2012, 24, 1762−1770

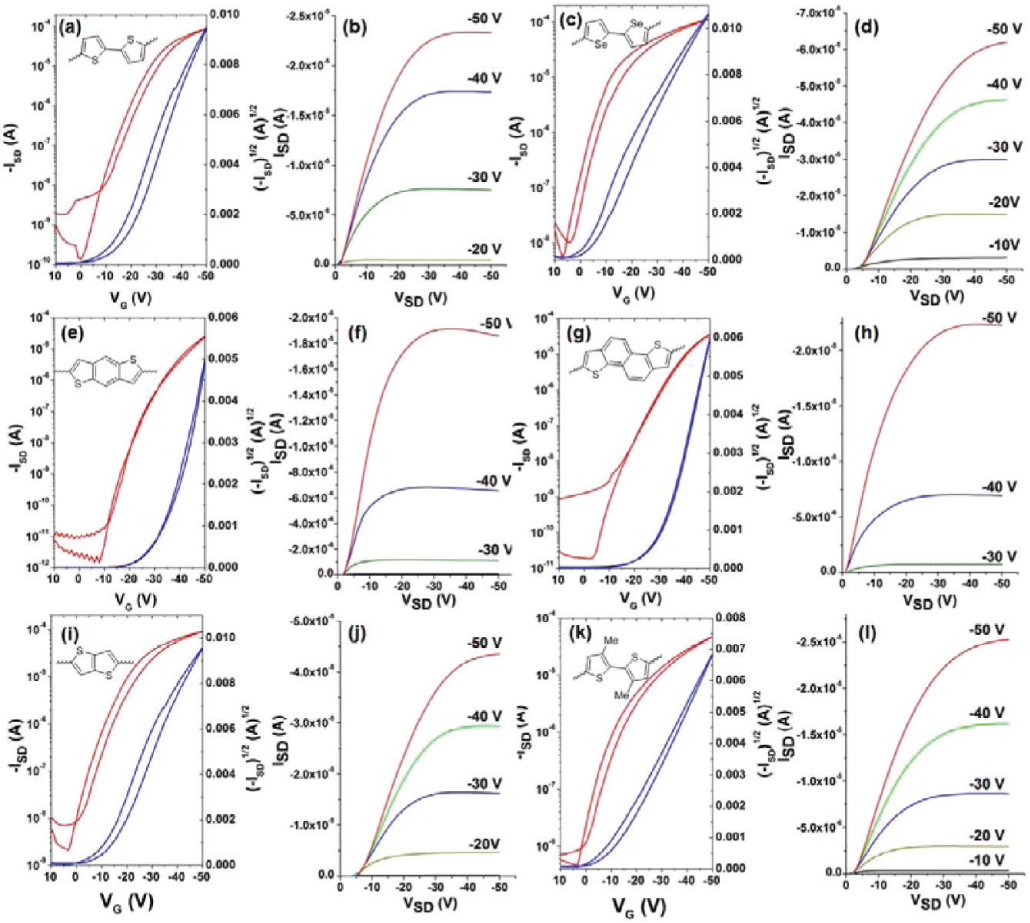

Figure 5. Transfer and output characteristics of (a, b) **IIDDT**, (c, d) **IID-Se**, (e, f) **IID-BDT**, (g, h) **IID-NDT**, (i, j) **IID-TT**, and (k, l) **IIDDT-Me** devices (spin-casted from TCB or TCE solutions, 4 mg/mL) at V_{SD} = −50 V (L = 60 μm, W = 3.0 mm) after thermal annealing.

Table 2. Bottom-Gate/Top-Contact (BG/TC) OFET Device Performances for Isoindigo-Based Polymers Measured under Ambient Condition (R_H = 50−60%)

polymers	$T_{annealing}$ (°C)	μ (cm^2 V^{-1} s^{-1})[a]	V_t (V)	I_{on}/I_{off}
IIDDT[b]	150	1.06 (0.66)	−18	10^6−10^7
IID-Se[b]	160	0.66 (0.46)	−10	10^5−10^6
IID-BDT[c]	150	0.48 (0.37)	−28	10^6−10^7
IID-NDT[b]	200	0.32 (0.25)	−30	10^6−10^7
IID-TT[c]	150	0.34 (0.31)	−6	10^5−10^6
IIDDT-Me[c]	150	0.11 (0.091)	−5	10^5−10^6
IIDT[c]	150	0.019 (0.015)	−20	10^5
IID-T3[c]	150	0.061 (0.048)	−4	10^5
IID-TTT[c]	200	1.03 × 10^{-3}	−4	10^4
IID-TBT[c]	150	1.35 × 10^{-4}	−16	10^3

[a]Maximum values of hole mobility and average mobilities are shown in parentheses (more than 10 devices were tested for each polymer). [b]Devices were fabricated using TCB as solvent without solvent annealing. [c]Devices were fabricated using TCE as solvent, and annealed in TCE solvent atmosphere for 2 h.

IID-BDT and −30 V for **IID-NDT**). This correlation is related to the hole-injection barrier from the gold electrode to the organic semiconducting layer. Gold electrode has a work function of 5.1 eV, and lowering the HOMO levels of polymers increase the barrier. Hence threshold voltages became more negative. **IID-BDT** and **IID-NDT** showed threshold voltages up to −30 V, nonetheless, their mobilities were high (0.48 cm^2 V^{-1} s^{-1} for **IID-BDT** and 0.32 cm^2 V^{-1} s^{-1} for **IID-NDT**). Interestingly these two polymers show very small hysteresis in transfer characteristics, indicating less trapping in polymer films.[5]

Note that **IIDDT** exhibit good stability for six months under ambient condition (see Figure S4 in the Supporting Information). After the storage, only a slight increase of the off-current was observed. Other centrosymmetric polymers (**IID-Se**, **IID-TT**, and **IIDDT-Me**) were stable under this condition for 2 months (see Figure S4 in the Supporting Information). All isoindigo polymers show good ambient stability, which may be attributed to their low-lying HOMO levels.[5]

Film Morphology and Molecular Packing. Tapping-mode atomic force microscopy (TM-AFM) was employed to investigate morphologies of polymer films. Figure 6 and Figure S5 in the Supporting Information show height images of polymer films prepared under the same condition as their device fabrications. Root-mean-square (rms) analyses of height images are also employed to reflect the roughness of films. Thermal annealing at 150 °C for 30 min resulted in negligible change in film morphologies. All polymers with centrosymmetric units, even **IIDDT-Me**, showed obviously crystallized zones or fibrillar intercalating networks in films. These networks were likely due to good intermolecular packing as observed in other high performance PFET materials.[2d,3] In contrast, polymers with axisymmetric units showed almost smooth and amorphous films. Polymers with centrosymmetric

dx.doi.org/10.1021/cm300117x | Chem. Mater. 2012, 24, 1762−1770

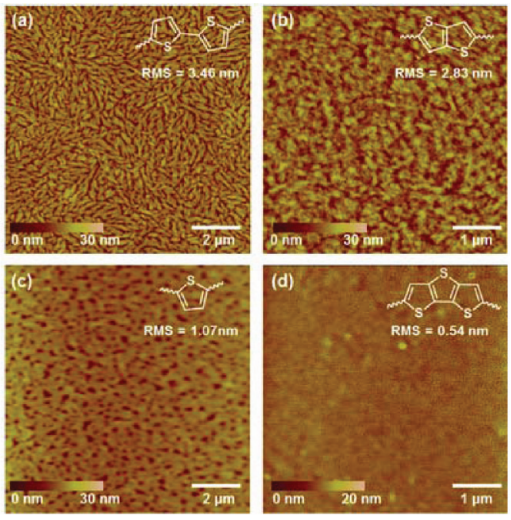

Figure 6. Tapping-mode AFM height images of (a) **IIDDT**, (b) **IID-BDT**, (c) **IIDT**, and (d) **IID-TTT** films spin-casted from TCE solution (4 mg/mL) on OTS-treated SiO_2/Si substrate and annealed at 150 °C for 30 min.

donors had higher surface roughness (3.46 nm for **IIDDT** and 2.83 nm for **IID-TT**) than those with axisymmetric donors (1.07 nm for **IIDT** and 0.54 nm for **IID-TTT**).

To understand the device performances from a molecular level, we employed GIXD to investigate polymer packing in thin film. Figure 7 shows the two-dimensional GIXD (2D-GIXD) patterns of polymer films prepared by spin-casting the TCE solution of polymers onto OTS-treated SiO_2/Si substrate. **IIDDT** and **IIDT-Se** films showed four out-of-plane diffraction peaks as spin-casted from their TCE solutions, which were attributed to 100, 200, 300, and 400 diffractions. After the films were thermally annealed at 150 °C for 30 min, the intensity of diffraction peaks increased, and diffraction points became more centered. **IID-BDT** and **IID-NDT** showed only three diffraction peaks before annealing, but after being annealed the fourth-order diffraction peaks appeared. Although these polymer films are relatively more amorphous than P3HT films, they also had ordered packing that was perpendicular to the film plane. According to the out-of-plane GIXD, first diffraction peaks of **IIDDT**, **IIDDT-Se**, **IID-BDT**, and **IID-NDT** were very strong at 2θ of 3.58, 3.60, 3.59, and 3.65°, corresponding to a *d*-spacing of 19.85, 19.74, 19.79, and 19.46 Å, respectively. These results are consistent with molecular models that polymer films had an edge-on lamellar packing in film. Only three diffraction peaks were observed for **IIDDT-Me** after thermal annealing and the 100 diffraction became much broader compared to that of **IIDDT**, indicating a relatively disordered lamellar packing. Presumably the methyl groups in **IIDDT-Me** hindered the interpolymer $\pi-\pi$ stacking, which may deteriorate out-of-plane lamellar packing. In sharp contrast, all polymers containing axisymmetric donor showed poor lamellar packing. **IID-T3** only displayed one diffraction peak, and the peak of **IIDT** was weak (Figure 7k, l, and Figure S7 in the Supporting Information). Polymers **IID-TTT** and **IID-TBT** showed no obvious diffraction peak. Interestingly, the first diffraction peak of **IIDT** was at 2θ of 3.25°, corresponding to a *d*-spacing of 21.86 Å, significantly larger than those of the centrosymmetric polymers.

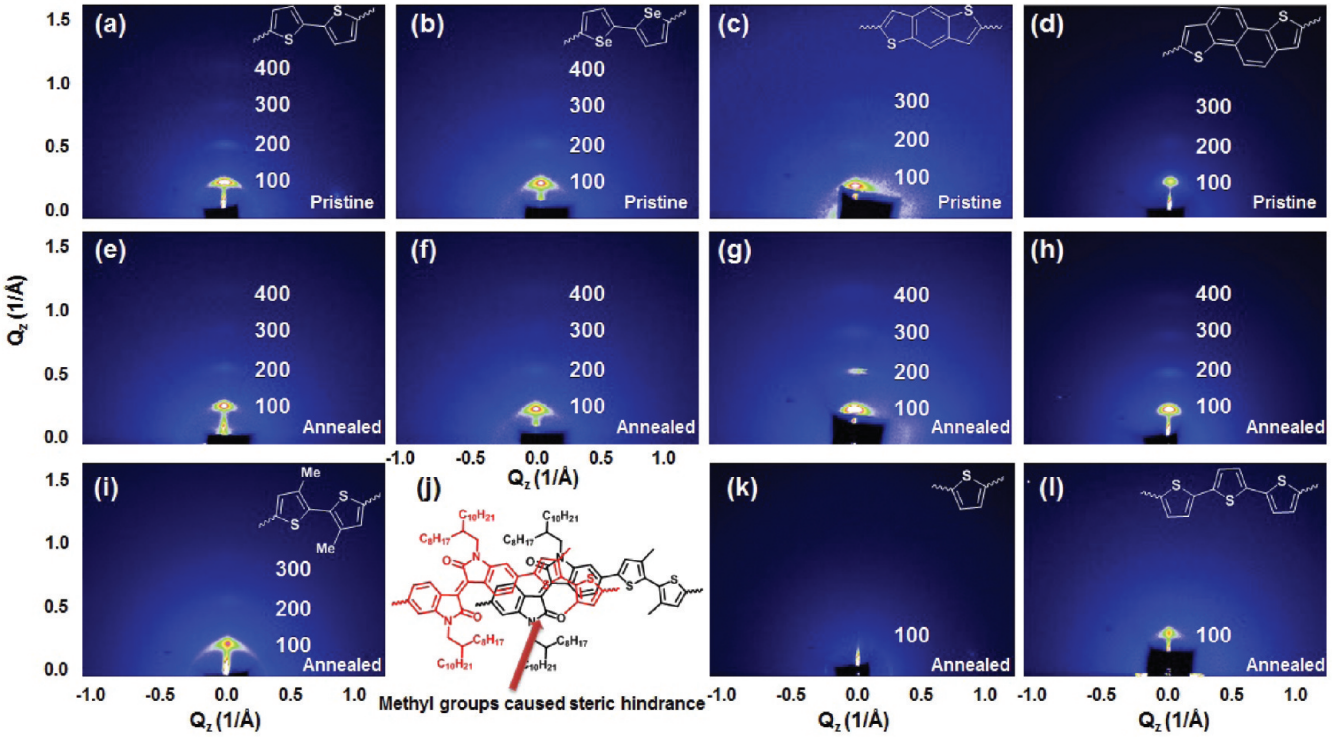

Figure 7. 2D-GIXD patterns of (a, e) **IIDDT**, (b, f) **IID-Se**, (c, g) **IID-BDT**, (d, h) **IID-NDT**, (i) **IIDDT-Me**, (k) **IIDT**, and (l) 6 in. thin films on OTS-treated SiO_2/Si substrate (all polymers were spin-coated from 8 mg/mL TCE solution followed by solvent annealing). (a–d) spin-cast film without thermal annealing and (e–i, k, l) annealed at 150 °C for 30 min at nitrogen atmosphere. (j) Schematic representation of the steric hindrance of **IIDDT-Me** for molecular docking.

dx.doi.org/10.1021/cm300117x | *Chem. Mater.* 2012, 24, 1762–1770

To further demonstrate our proposed packing model of polymers, we performed ab initio DFT calculations. Specifically, ωB97X-D functional, which includes empirical dispersion, was used in order to correctly describe the weak intermolecular interaction.[23] Long alkyl chains were replaced with isobutyl groups. We used oligomers (n = 2) of **IIDDT** to explore the $\pi-\pi$ stacking of two polymer chains and several local minimum structures were found from different starting structures. Direct overlap of isoindigo cores exhibited much higher energy because the strong repulsion caused by alkyl chains. The most stable intermolecular stacking is shown in Figure 8a and the association energy of the dimer is 55.1 kcal/mol. Bithiophene units partly overlapped with the isoindigo cores with $\pi-\pi$ stacking distances in the range of 3.4−3.5 Å. These results agreed with the absorption spectra that the polymer formed some *J*-aggregates in film. Figure 8b shows the electrostatic potential of the dimer. The HOMO of dimers was delocalized on both oligomers which indicated the strong interaction of their frontier orbitals (see Figure S8 in the Supporting Information). However, after incorporating methyl groups, oligomers of **IIDDT-Me** showed larger $\pi-\pi$ stacking distance, and the association energy was 49.9 kcal/mol, smaller than that of **IIDDT**. Interestingly, the $\pi-\pi$ stacking suppressed the torsion angles of **IIDDT-Me** from 29° to 7.8°, which is also consistent with the absorption spectra (see Figure S9 in the Supporting Information). Polymers with axisymmetric donor, such as **IIDT**, cannot form good $\pi-\pi$ stacking and the association energy of **IIDT** dimer was only 43.5 kcal/mol. The association energy among these three polymers will be much larger. Therefore, these computational results prove our molecular packing models and support the "molecular docking" strategy that small donor units can dock into large isoindigo cores to enhance interchain $\pi-\pi$ stacking.

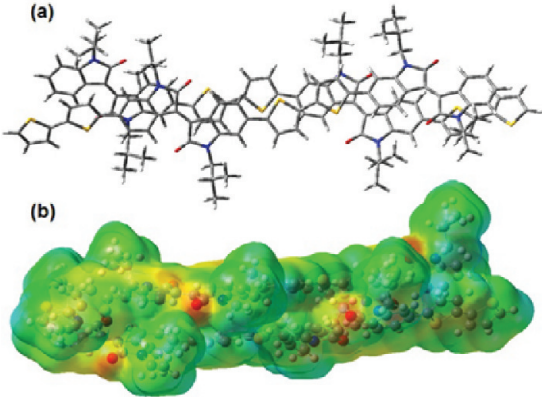

Figure 8. (a) Calculated dimer structures of the **IIDDT** oligomers (n = 2). Structural optimization was performed at ωB97X-D/6-31G(d) level. (b) Side view of the electrostatic potential of the dimer.

Molecular Docking Strategy. Figure 9a shows a cartoon representation of conjugated polymer films,[27] which is very similar to the film morphology of **IIDDT** (Figure 6a). In a typical polymer film, three possible carrier transporting pathways are marked with arrows: (1) intrachain carrier transport, which is very fast and efficient; (2) interchain carrier transport at well-ordered sites, which may adopt a hopping mechanism like ordered small molecules; (3) interchain carrier transport at loosely contacted sites, which is very slow. Therefore, the carrier transport is obviously limited by loosely contact sites, and improve the carrier mobility at pathway (3) is crucial for high-performance PFETs. One effective way to reduce zones of pathway (3) is to increase interpolymer chain interactions and thus increasing the polymer packing orders.

Traditional polymers designed for PFETs, such as P3HT, always contain one or two alkyl chains on each unit (Figure 9b). Typical alkanes (C_nH_{2n+2}) (n = 6−9) have inter alkyl chain distances of 3.6−3.8 Å in single crystal,[24] larger than a typical $\pi-\pi$ distance of 3.4 Å.[9,25] Hence, steric hindrance may exist

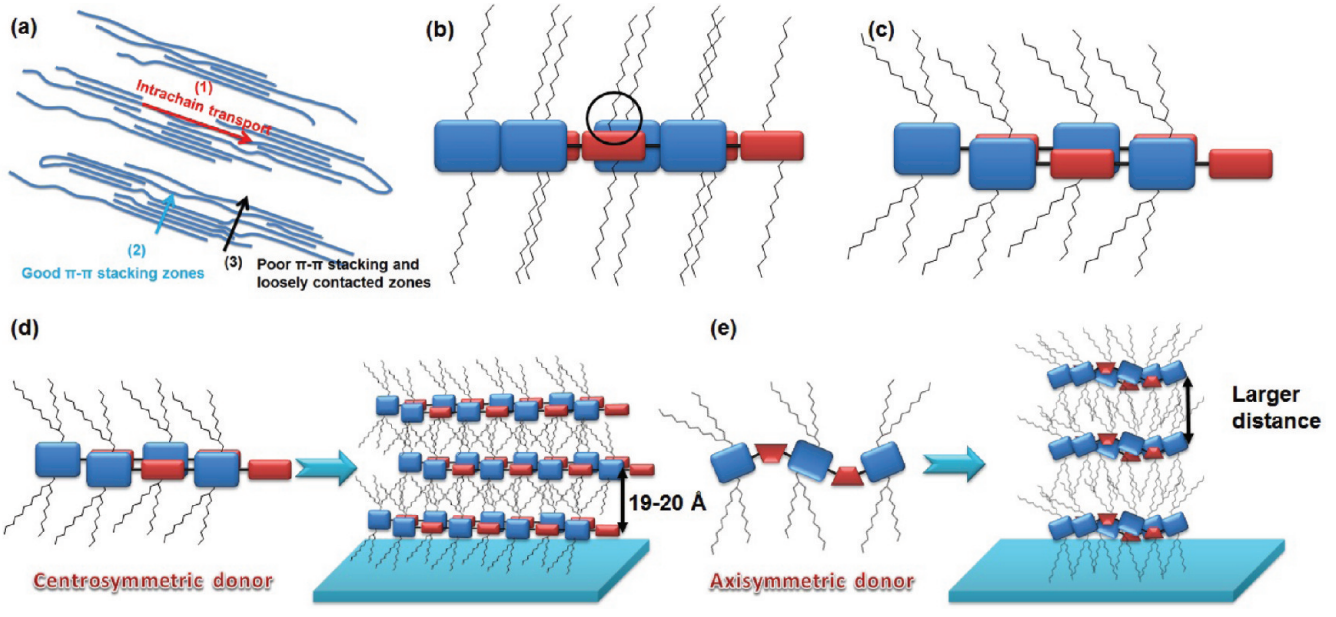

Figure 9. (a) Cartoon representation of conjugated polymer film, and its three possible charge transport pathways. (b) Traditional polymer contains one or two alkyl chains on each unit. Steric hindrance may exist when polymers are stacked with each other (black circle). (c) Molecular docking strategy to avoid steric hindrance and improve the interpolymer $\pi-\pi$ interaction. The cartoon representation of copolymers with different symmetries and their film packings; (d) polymers with centrosymmetric donors and (e) polymers with axisymmetric donors.

dx.doi.org/10.1021/cm300117x | *Chem. Mater.* 2012, 24, 1762−1770

Scheme 2. Diketopyrrolopyrole and Naphthalenedicarboximide-Based Large Aromatic Core Polymers and Their FET Performances

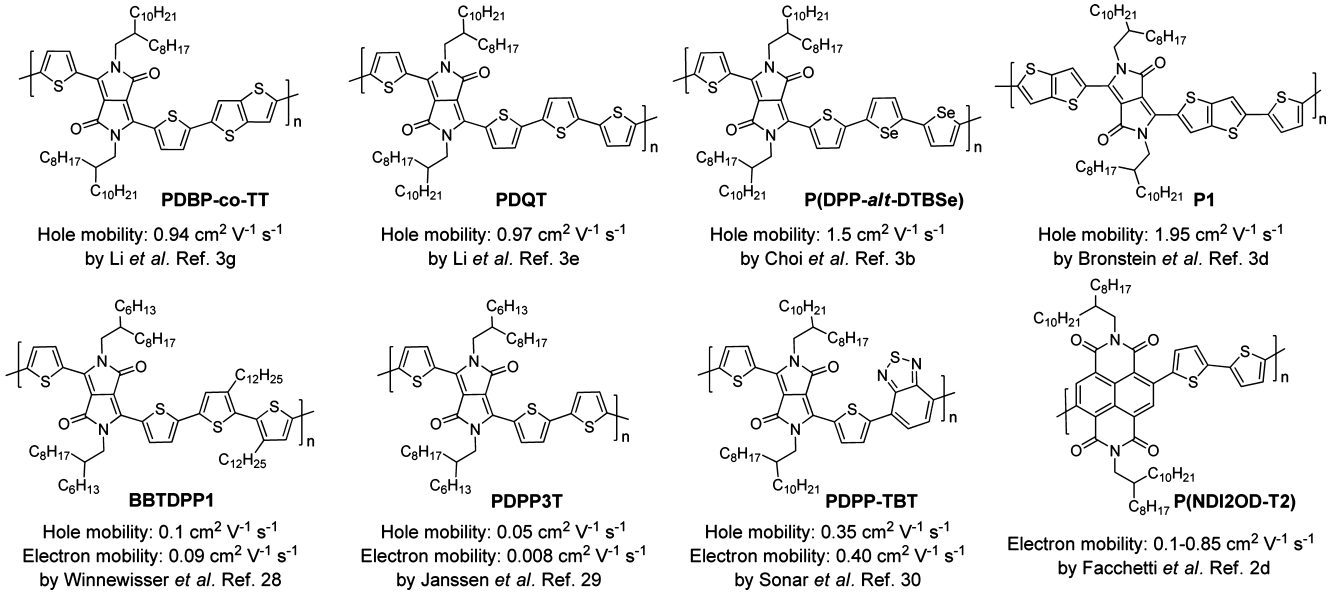

when polymers are stacked with each other. Removal of alkyl chains from small units will avoid this steric hindrance (Figure 9c). Starting from this rough analysis, we propose the molecular docking design strategy: (1) reducing the steric hindrance of alkyl chains and making the small unit "dock into" a large aromatic core, similar to the "brick layer" packing of TIPS-pentacene; (2) large aromatic core can also reduce reorganization energy of polymers, which has been widely used in the design of high-performance small molecule OFETs.[6,7]

As described above, device performances of the polymers apparently correlated with their film morphologies and polymer packings. Polymers with centrosymmetric units exhibited better crystallinity and lamellar packing in thin films, because of good interchain $\pi-\pi$ stacking. As shown in Figure 9d,e, for those polymers with centrosymmetric units, the "small unit" can readily dock into the cavity formed by the "large core" and branched alkyl chains. The donor−acceptor interaction between the isoindigo core and the donor unit further enhances the docking. In addition, the polymers backbones with centrosymmetric donors are almost linear and parallel to the substrate. The decent $\pi-\pi$ stacking and the linear backbone of polymers led to good lamellar phase in polymer films, as proved by GIXD experiment (Figure 9d). Even for methyl-substituted **IIDDT-Me**, the backbone remains linear. **IIDDT-Me** shows good lamellar packing yet poor maximum mobility (0.11 $cm^2\ V^{-1}\ s^{-1}$), presumably because of poor $\pi-\pi$ stacking caused by methyl groups.

Polymer backbones containing axisymmetric donors, nonetheless, become zigzag, inhibiting the docking and lamellar packing in polymer film, as shown in Figure 9e. With the most linear backbone, **IID-T3** shows the best hole-mobility up to 0.061 $cm^2\ V^{-1}\ s^{-1}$. This result indicates the importance of backbone curvature. The important effect of symmetry[26] and backbone curvature[16,27] on PFETs are also reported by other groups.

The "molecular docking" strategy is applicable to other systems, such as diketopyrrolopyrole (DPP)[3b,d,e,g,28−30] and naphthalenedicarboximide (NDI).[2d] Scheme 2 presents several recently developed polymers with mobilities around 1 $cm^2\ V^{-1}\ s^{-1}$. Polymers with centrosymmetric units, such as **PDBP-co-TT**, **PDQT**, **P(DPP-*alt*-DTBSe)** and n-type **P(NDI2OD-T2)**, showed excellent mobilities. In contrast, those with axisymmetric units and zigzag backbones (**PDP3T**[29] and **PDPP-TBT**[30]) had relatively low mobilities. Similar to **IID-T3**, although **P1** contains axisymmetric thiophenes, it has an almost linear backbone, thus showing good mobility. With an identical backbone to **PDQT** yet two additional dodecyl chains, **BBTDPP1**[28] showed hole mobility as high as 0.1 $cm^2\ V^{-1}\ s^{-1}$, almost 1 order of magnitude lower than **PDQT**. This example is comparable to **IIDDT-Me**.

CONCLUSION

In summary, we introduce the "molecular docking" strategy to design new polymers for high-performance PFETs. The key concept of molecular docking is that the small conjugated units can dock into the cavity formed by large aromatic cores and alkyl chains. This docking leads to increased interchain $\pi-\pi$ stacking of the polymer. According to the strategy, a series of isoindigo-based polymers have been designed and synthesized for high-performance PFETs. Excitingly, the molecular docking design provides us systematically high device performances. Six polymers with centrosymmetric units show hole-mobilities over 0.1 $cm^2\ V^{-1}\ s^{-1}$, in which five polymers show hole-mobilities over 0.3 $cm^2\ V^{-1}\ s^{-1}$. **IIDDT** gives a maximum hole-mobility over 1 $cm^2\ V^{-1}\ s^{-1}$. In addition, these polymers show good stability upon moisture due to low HOMO levels. By using AFM and GIXD analyses, we have attributed the obvious difference in device performance to the different symmetry and backbone curvature of polymers, which greatly affect the interchain $\pi-\pi$ stacking, lamellar packing and crystallinity. Furthermore, DFT calculations support our proposed packing model and the molecular docking strategy. Finally, we compare the device performances of several DPP and NDI based polymers reported by other groups, and find that the molecular docking strategy is also applicable in their systems. The molecular docking strategy is effective and general in polymer design for PFETs. We are currently extending this strategy to other systems with large aromatic cores.

dx.doi.org/10.1021/cm300117x | Chem. Mater. 2012, 24, 1762−1770

■ ASSOCIATED CONTENT

Supporting Information

Monomers/polymers synthesis, characterization, and device fabrication details. This material is available free of charge via the Internet at http://pubs.acs.org.

■ AUTHOR INFORMATION

Corresponding Author

*E-mail: jianpei@pku.edu.cn (J. Pei).

Notes

The authors declare no competing financial interest.

■ ACKNOWLEDGMENTS

This work was supported by the Major State Basic Research Development Program (No 2009CB623601) from the Ministry of Science and Technology, and National Natural Science Foundation of China. We thank Prof. Xiao-Yu Cao (Xiamen University) for his suggestion and insightful discussion. The authors thank beamline BL14B1 (Shanghai Synchrotron Radiation Facility) for providing the beam time.

■ REFERENCES

(1) (a) Katz, H. E. *Chem. Mater.* **2004**, *16*, 4748. (b) Zaumseil, J.; Sirringhaus, H. *Chem. Rev.* **2007**, *107*, 1296. (c) Tang, Q.; Jiang, L.; Tong, Y.; Li, H.; Liu, Y.; Wang, Z.; Hu, W.; Liu, Y.; Zhu, D. *Adv. Mater.* **2008**, *20*, 2947. (d) Wen, Y.; Liu, Y. *Adv. Mater.* **2010**, *22*, 1331. (e) Guo, Y.; Yu, G.; Liu, Y. *Adv. Mater.* **2010**, *22*, 4427.

(2) (a) Garnier, F.; Hajlaoui, R.; Yassar, A.; Srivastava, P. *Science* **1994**, *265*, 1864. (b) Sirringhaus, H.; Tessler, N.; Friend, R. H. *Science* **1998**, *208*, 1741. (c) Sirringhaus, H.; Kawase, T.; Friend, R. H.; Shimoda, T.; Inbasekaran, M.; Wu, W.; Woo, E. P. *Science* **2000**, *290*, 2123. (d) Yan, H.; Chen, Z.; Zheng, Y.; Newman, C.; Quinn, J. R.; Doltz, F.; Kestler, M.; Facchetti, A. *Nature* **2009**, *457*, 679.

(3) (a) Guo, X.; Ortiz, R. P.; Zheng, Y.; Kim, M.-G.; Zhang, S.; Hu, Y.; Lu, G.; Facchetti, A.; Marks, T. J. *J. Am. Chem. Soc.* **2011**, *133*, 13685. (b) Ha, J. S.; Kim, K. H.; Choi, D. H. *J. Am. Chem. Soc.* **2011**, *133*, 10364. (c) Lei, T.; Cao, Y.; Fan, Y.; Liu, C.-J.; Yuan, S.-C.; Pei, J. *J. Am. Chem. Soc.* **2011**, *133*, 6099. (d) Bronstein, H.; Chen, Z.; Ashraf, R. S.; Zhang, W.; Du, J.; Durrant, J. R.; Tuladhar, P. S.; Song, K.; Watkins, S. E.; Geerts, Y.; Wienk, M. M.; Janssen, R. A. J.; Anthopoulos, T.; Sirringhaus, H.; Heeney, M.; McCulloch, I. *J. Am. Chem. Soc.* **2011**, *133*, 3272. (e) Li, Y.; Sonar, P.; Singh, S. P.; Soh, M. S.; van Meurs, M.; Tan, J. *J. Am. Chem. Soc.* **2011**, *133*, 2198. (f) Tsao, H. N.; Cho, D. M.; Park, I.; Hansen, M. R.; Mavrinskiy, A.; Yoon, D. Y.; Graf, R.; Pisula, W.; Spiess, H. W.; Müllen, K. *J. Am. Chem. Soc.* **2011**, *133*, 2605. (g) Li, Y.; Singh, S. P.; Sonar, P. *Adv. Mater.* **2010**, *22*, 4862.

(4) Sirringhaus, H. *Adv. Mater.* **2009**, *21*, 3859.

(5) (a) Osaka, I.; Sauve, G.; Zhang, R.; Kowalewski, T.; McCullough, R. D. *Adv. Mater.* **2007**, *19*, 4160. (b) Osaka, I.; Zhang, R.; Sauve, G.; Smilgies, D.-M.; Kowalewski, T.; McCullough, R. D. *J. Am. Chem. Soc.* **2009**, *131*, 2521. (c) Osaka, I.; Zhang, R.; Liu, J.; Smilgies, D.-M.; Kowalewski, T.; McCullough, R. D. *Chem. Mater.* **2010**, *22*, 4191. (d) Osaka, I.; Takimiya, K.; McCullough, R. D. *Adv. Mater.* **2010**, *22*, 4993.

(6) Coropceanu, V.; Jérôme, C.; da Silva Filho, D. A.; Olivier, Y.; Silbey, R.; Brédas, J.-L. *Chem. Rev.* **2007**, *107*, 926.

(7) Takimiya, K.; Shinamura, S.; Osaka, I; Miyazaki, E. *Adv. Mater.* **2011**, *23*, 4347.

(8) (a) Anthony, J. E. *Angew. Chem., Int. Ed.* **2008**, *47*, 452. (b) Anthony, J. E. *Chem. Rev.* **2006**, *106*, 5028.

(9) Sokolov, A. N.; Atahan-Evrenk, S.; Mondal, R.; Akkerman, H. B.; Sánchez-Carrera, R. S.; Granados-Focil, S.; Schrier, J.; Mannsfeld, S. C. B.; Zoombelt, A. P.; Bao, Z.; Aspuru-Guzik, A. *Nature Commun.* **2011**, *2*, 437.

(10) Höltje, H.-D.; Folkers, G. *Molecular Modeling: Basic Principles and Applications*; Wiley-VCH: Weinheim, Germany, 1996.

(11) Kitchen, D. B.; Decornez, H.; Furr, J. R.; Bajorath, J. *Nat. Rev. Drug Discovery* **2004**, *3*, 935.

(12) (a) Wang, E.; Ma, Z.; Zhang, Z.; Vandewal, K.; Henriksson, P.; Inganäs, O.; Zhang, F.; Andersson, M. R. *J. Am. Chem. Soc.* **2011**, *133*, 14244. (b) Zhang, G.; Fu, Y.; Xie, Z.; Zhang, Q. *Macromolecules* **2011**, *44*, 1414. (c) Mei, J.; Graham, K. R.; Stalder, R.; Reynolds, J. R. *Org. Lett.* **2010**, *12*, 660. (d) Stalder, R.; Mei, J.; Reynolds, J. R. *Macromolecules* **2010**, *43*, 8348.

(13) Stalder, R; Mei, J. G.; Subbiah, J.; Grand, C.; Estrada, L. A.; So, F.; Reynolds, J. R. *Macromolecules* **2011**, *44*, 6303.

(14) Guo, X. G.; Watson, M. D. *Org. Lett.* **2008**, *10*, 5333.

(15) Chen, Z.; Zheng, Y.; Yan, H.; Facchetti, A. *J. Am. Chem. Soc.* **2009**, *131*, 8.

(16) Rieger, R.; Beckmann, D.; Mavrinskiy, A.; Kastler, M.; Müllen, K. *Chem. Mater.* **2010**, *22*, 5314.

(17) Osaka, I.; Abe, T; Shinamura, S.; Miyazaki, E.; Takimiya, K. *J. Am. Chem. Soc.* **2010**, *132*, 5000.

(18) Sato, M.; Asami, A.; Maruyama, G.; Kosuge, M.; Nakayama, J.; Kumakura, S.; Fujihara, T.; Unoura, K. *J. Organomet. Chem.* **2002**, *654*, 56.

(19) Li, J.; Qin, F.; Li, C. M.; Bao, Q.; Chan-Park, M. B.; Zhang, W.; Qin, J.; Ong, B. S. *Chem. Mater.* **2010**, *22*, 5314.

(20) Rieger, R.; Beckmann, D.; Pisula, W.; Steffen, W.; Kastler, M.; Müllen, K. *Adv. Mater.* **2010**, *22*, 83.

(21) Majewski, L. A.; Kingsley, J. W.; Balocco, C.; Songa, A. M. *App. Phys. Lett.* **2006**, *88*, 222108.

(22) Chang, J.-F.; Clark, J.; Zhao, N.; Sirringhaus, H.; Breiby, D. W.; Andreasen, J. W.; Nielsen, M. M.; Giles, M.; Heeney, M.; McCulloch, I. *Phys. Rev. B* **2006**, *74*, 115318.

(23) Cha, D.; Head-Gordon, M. *Phys. Chem. Chem. Phys.* **2008**, *10*, 6615.

(24) Boese, R.; Weiss, H. C.; Bläser, D. *Angew. Chem., Int. Ed.* **1999**, *38*, 988.

(25) (a) Liang, Z.; Tang, Q.; Xu, J.; Miao, Q. *Adv. Mater.* **2011**, *23*, 1535. (b) Lei, T.; Zhou, Y.; Cheng, C.-Y.; Cao, Y.; Peng, Y.; Bian, J.; Pei, J. *Org. Lett.* **2011**, *13*, 2642. (c) Liu, Y.-Y.; Song, C.-L.; Zeng, W.-J.; Zhou, K.-G.; Shi, Z.-F.; Ma, C.-B.; Yang, F.; Zhang, H.-L.; Gong, X. *J. Am. Chem. Soc.* **2010**, *132*, 16349.

(26) He, M.; Li, J.; Tandia, A.; Sorensen, M.; Zhang, F.; Fong, H. H.; Pozdin, V. A.; Smilgies, D.-M.; Malliaras, G. G. *Chem. Mater.* **2010**, *22*, 2770.

(27) Osaka, I.; Abe, T.; Shinamura, S.; Takimiya, K. *J. Am. Chem. Soc.* **2011**, *133*, 6852.

(28) Burgi, L.; Turbiez, M.; Pfeiffer, R.; Bienewald, F.; Kirner, H.-J.; Winnewisser, C. *Adv. Mater.* **2008**, *20*, 2217.

(29) Bijleveld, J. C.; Zoombelt, A. P.; Mathijssen, S. G. J.; Wienk, M. M.; Turbiez, M.; Leeuw, D. M.; Janssen, R. A. J. *J. Am. Chem. Soc.* **2009**, *131*, 16616.

(30) Sonar, P.; Singh, S. P.; Li, Y.; Soh, M. S.; Dodabalapur, A. *Adv. Mater.* **2010**, *22*, 5409.